*Paper presented at the Third International Conference on Nuclear Microprobe Technology and Applications, Uppsala, June 1992.*

# $He^+$ and H+ Microbeam Damage, Swelling and Annealing in Diamond.

**Sean P. Dooley, David N. Jamieson and Steven Prawer.**

*Micro Analytical Research Centre, School of Physics,*
*University of Melbourne, Parkville 3052, AUSTRALIA.*

The effects of scanned 2 MeV $He^+$ and 1.4 MeV $H^+$ microbeam irradiation on unimplanted and P implanted diamond were characterized. Although diamond was found to be resistant to lattice defect production, it was found to swell very rapidly in comparison with other materials, giving rise to serious swelling induced dechanneling at scan edges [1] at relatively low doses ($10^{17}/cm^2$ for 2 MeV $He^+$). Microbeams annealed the damage due to a 1.5 $\mu$m deep Phosphorus implantation at a dose of $10^{15}P^+/cm^2$. The implantation damage was reduced at a dose of ($1.6 \times 10^{17}/cm^2$) by up to 21 % for 2 MeV $He^+$ irradiation, up to 16 % for high flux 1.4 MeV $H^+$ irradiation and 12 % for low flux $H^+$ irradiation. For the choice of analysis beam, all these beam effects were found to be most significant for $He^+$ microbeams, so $H^+$ microbeams should be used for analysis of diamond unless high depth resolution is required.

## Introduction.

Ion microprobes can allow large doses ($\sim 10^{17}/cm^2$) to be applied to small regions ($\sim 50\mu m$) at high fluxes ($\sim 20\mu A/cm^2 = 2.0 \times 10^{14} ions/cm^2/s$ ), making them an ideal tool for studying high dose ion irradiation effects in materials, such as swelling and ion beam annealing.

Microprobes are also used as analytical instruments, to obtain channeling and compositional information on a micron-sized scale, where analysis conditions must be used that strictly limit the effects of the analysis beam on the measurement. Under microbeam irradiation, lattice defects can form [1–4], dopants can be displaced from lattice sites [2],

and swelling can misorient the edge of the irradiated region, inducing dechanneling [1]. It is known that high energy light ions can anneal damage produced by heavy ion irradiation [5], and this is a potential source of analysis beam induced specimen perturbation for microprobe analysis of ion implanted crystal.

Light ion microprobe analysis is a useful technique for characterizing dopant ion implantation damage and the success of spot annealing treatments [6–8]. In our current work, 1.5 $\mu$m deep Carbon or Phosphorus implants in type IIa natural diamond slabs are annealed by a focussed, pulsed Nd-Glass laser. This process produces small ($\sim 10\mu$m) spots of annealed diamond which have been successfully analyzed by a scanned 1.4 MeV $H^+$ microbeam [7,8]. In order to ensure that significant changes to the crystal under analysis did not occur, it was necessary to perform systematic damage studies on unimplanted diamond to characterize lattice damage and swelling induced dechanneling, and implanted diamond to characterize possible annealing effects.

## 1. Lattice Damage and Swelling Induced Dechanneling.

Lattice damage in diamond due to 1 MeV $He^+$ irradiation has been found to cause measurable loss of channeling at the diamond surface, [9] as well as significant damage at the end of range. Also, we have previously investigated [1] the loss of channeling in Si crystal irradiated by 2 MeV $He^+$ in small scans ($\sim 100 \times 100\mu$m), typical of microprobe channeling measurements [1]. Beam induced swelling was found to be the only significant cause of dechanneling at high doses in Si. To accommodate the swelling induced by the buildup of defects and beam atoms at the end of range, the crystal layers at the edge of the irradiated region must be tilted. A tilt of $\sim 0.5°$ is enough to cause severe dechanneling at the scan edge.

As the present work shows, diamond swells more readily than Si under ion irradiation, despite its hardness, so swelling induced dechanneling was expected to occur at lower doses. Previous work carried out with 170 keV fluorine beams [10] attributed this swelling to the buildup of vacancies at the end of range of the beam, which gives an initially rapid component of swelling that eventually saturates, and the accommodation of the implanted ions in the lattice, which gives a linear component of swelling with dose. The diamond at

the end of range of the beam is not converted to graphite [10], but it appears black due to $sp_2$ bond formation.

### 1.1 Experimental.

A detailed investigation was carried out on the effect of microprobe irradiation of unimplanted diamond. High dose irradiations of <110> oriented unimplanted type IIa diamond were performed with channeled 1.4 MeV $H^+$ and 2 MeV $He^+$ beams at room temperature to characterize lattice damage, swelling, and swelling induced dechanneling in diamond. The combination of these two effects we refer to as 'channeling loss'.

The energy of 2 MeV for $He^+$ was chosen, as this is the routine energy used at the Melbourne University Microprobe for channeling, and is the energy used in nearly all of the microprobe damage literature. The proton energy of 1.4 MeV was chosen because it has approximately the same critical angle for channeling (0.36°) as a 2 MeV $He^+$ beam [9], giving comparable results to the $He^+$ beam.

Raman Spectroscopy, Dektak surface profiles and Channelling Contrast Microscopy (CCM) [6], were used in the characterization of damage and swelling.

### 1.2 Characterization of Swelling.

The swelling produced in diamond by microprobe scans typically used in the analysis of microscopic features [7,8] was investigated. A region of <110> oriented unimplanted diamond was irradiated in a $32 \times 32 \mu$m square by a scanned 1.4 MeV $H^+$ beam in channeling orientation to a dose of $5 \times 10^{17}/cm^2$. The surface was swollen to a height of 60 nm as is shown in the Dektak profilometer trace (figure 1). From the Young's modulus of diamond ($1.05 \times 10^{12}$Pa), and the range of the beam ($17 \pm 2 \mu$m, based on a c-STIM measurement [11] of the energy loss of 1 MeV $H^+$ in channeling orientation in Si), the stress at the end of range of the beam required to produce the observed swelling is calculated to be $3.7 \pm 0.5$ GPa. Following the microprobe irradiation, Raman spectroscopy was performed on this region. A Raman peak shift of 8.2 $cm^{-1}$ from the Raman peak of virgin diamond was measured for the swollen region (figure 2). The Raman peak of the swollen region was also

broadened. The average tensile stress could thus be found to be 4.0 GPa in the surface region of the swelling, which is consistent with the end of range stress calculated from the observed swelling height.

The swelling height was measured for all of the scans used in this study. For 2 MeV $He^+$ irradiation, the surface swelling (723 nm at a dose of $3.7 \times 10^{17}/cm^2$) was over 11 times greater than that for 1.4 MeV proton irradiation and 3 times greater than that observed for 170 keV fluorine irradiation [10], at this dose. The larger amount of swelling per ion observed for $He^+$ irradiation is due partially to the higher defect production rate of the beam (compared to $H^+$), and also possibly due to the fact that He cannot combine chemically with lattice defects, while both H and F can combine with the dangling bonds of lattice vacancies. The fact that diamond swells four times more than silicon [1] per unit $He^+$ dose is probably due to the smaller lattice spacing of diamond which means that there is more stress induced by an interstitial He or C atom.

### 1.3 Characterization of 1.4 MeV $H^+$ Channelling Loss.

To investigate the microbeam induced swelling, CCM images were taken at various stages of irradiation for a $67 \times 67 \mu m$ square of unimplanted diamond irradiated at a flux of 18 $\mu A/cm^2$ to a maximum dose of $6.1 \times 10^{17}/cm^2$. Spectra extracted from the centres of these scans give information on the lattice damage due to the beam, and spectra extracted from the edges of the images give the swelling induced dechanneling effect of the irradiation.

A CCM image (figure 3) of the irradiated region was taken with the 67 $\mu m$ scan after the irradiation of the $67 \mu m$ region to a dose of $6.1 \times 10^{17}/cm^2$. The only visible features in this image are due to the effects of the 67 $\mu m$ scanned beam. It is clear that there was significant dechanneling at the edge of the scan, which gives rise to an increase in total $\chi_{min}$ measured with that scan. A CCM image of this region taken with a larger scan showed little contrast between the centre of the irradiated region and the unirradiated background, indicating negligible buildup of lattice damage.

To definitely establish swelling induced dechanneling as the mechanism for the loss of contrast at the edge of the irradiated region, a CCM image (figure 4) of the left edge of

the swollen region as in figure 3 was taken at an angle of 0.5° to the channeling axis. The channeling feature in this image corresponds to an edge of the swelling produced by the $67 \times 67\mu$m scan. This confirms that the edge was misoriented by swelling as has been previously observed in Si [1]. A Dektak measurement of the $67\mu$m irradiated region showed a surface swelling of 165 nm at the maximum dose of $6.1 \times 10^{17}/\text{cm}^2$, which is approximately twice the swelling observed in Si at the same $H^+$ dose [12].

The $\chi_{min}$ is plotted as a function of dose (figure 5) for the 0.8 nA 1.4 MeV $H^+$ beam scanned in the $67 \times 67\mu$m square. The $\chi_{min}$ was measured in the centre and at the edge of the scan used to produce the damage, as well as for the entire scan. The $\chi_{min}$ in the centre of the scan does not increase, indicating a negligible rate of buildup of lattice damage in the surface region of the crystal. The $\chi_{min}$ of the edge gradually increases after a dose of $1.5 \times 10^{17}/\text{cm}^2$ due to tilting caused by swelling. The crystal is otherwise undamaged.

### 1.4 Characterization of 2 MeV $He^+$ Channelling Loss.

The $\chi_{min}$ was measured by CCM imaging as a function of dose for a 2 MeV $He^+$ beam scanned in a $108 \times 108\mu$m square. The $\chi_{min}$ is plotted as a function of dose (figure 6) for the entire scan, the scan centre, and the edge of the scan. The $\chi_{min}$ in the centre of the scan does not increase, but the $\chi_{min}$ of the edge rapidly increases after a dose of $1.0 \times 10^{17}/\text{cm}^2$ to 30 % due to swelling induced dechanneling, and then increases more slowly. This result indicates that the beam produces negligible lattice damage at the surface, which is at variance with the previous study [9], but insufficient information on that experiment was given to allow us to explain the apparent discrepancy.

## 2. Microbeam Annealing of Ion Implanted Diamond.

In a previous study of the effects of $H^+$ and $He^+$ irradiation of Sb implanted in diamond to a dose of $1 \times 10^{14}/\text{cm}^2$ [5], the damage could be annealed to an equilibrium level of 46 % of its initial level by channeled 2.3 MeV $He^+$ at a dose of $1.5 \times 10^{17}/\text{cm}^2$, and 320 keV $H^+$ could anneal the damage to an equilibrium value of 60 %. Thus for channeling analysis of ion implanted diamond, annealing effects due to the analysis beam potentially pose a considerable problem.

## 2.1 Experimental.

A <110> diamond wafer was implanted with Phosphorus to a range of 1.5 $\mu$m at a dose of $1 \times 10^{15} P^+/cm^2$ to determine whether the laser annealing technique developed in [7] could activate the dopant [8]. It was necessary to ensure that annealing effects of the 1.4 MeV $He^+$ beam used for the microchanneling analysis of the laser annealed spots were minimized.

High dose irradiations along the <110> axis of the implanted diamond were performed with 1.4 MeV $H^+$ and 2 MeV $He^+$ beams at room temperature to characterize the annealing effects of the beams. The level of damage was measured by integrating over the damage distribution and subtracting the channeling yield from unimplanted diamond over that same depth region. This measurement contains both direct scatter and dechanneling effects of the damage, but is approximately proportional to the defect concentration. The level of damage is expressed as a fraction of the initial implantation damage.

## 2.2 Proton Beam Annealing of P implanted diamond.

A 67 $\mu$m square region of the implanted diamond was irradiated at room temperature by a 1.4 MeV $H^+$ beam in the <110> channeling orientation at a beam flux of $5.6 \times 10^{16}/cm^2$. The maximum dose used was $3.7 \times 10^{17}/cm^2$.

From the CCM image (figure 8) of the irradiated region, obtained with a 135 $\mu$m square scan, it is possible to see that there is slightly better channeling into the scan centre than into the unirradiated material at the edge of the image. Around the centre of the image, corresponding to the edge of the original 67 $\mu$m square scan, is a region of poor channeling due to swelling induced dechanneling. This irradiation was found to have produced a swelling of 65 nm as measured by the Dektak surface profilometer.

The channeling spectra for the P implanted layer at $H^+$ doses of $7.0 \times 10^{15}/cm^2$ (as implanted) and $3.7 \times 10^{17}/cm^2$ (ion beam annealed) are shown (figure 9), together with the spectrum for unimplanted diamond. The high dose anneals the damage by 15 %. The spectrum for the dose of $3.7 \times 10^{17}/cm^2$ was extracted from the centre of the irradiated

region to eliminate swelling effects.

As defect production in ion beam irradiated materials is highly flux dependent [2] due to dynamic annealing processes [3], it was anticipated that annealing could also be flux dependent. Another 1.4 MeV $H^+$ damage study was performed at over 10 times the previous flux to investigate this possibility. The focused microbeam was scanned in a $40 \times 30 \mu$m rectangle at an average beam current of 0.75 nA in channeling orientation, giving a flux of $63 \mu A/cm^2$. Although doses above $1.7 \times 10^{17}/cm^2$ could not be used due to swelling induced dechanneling, it was found that the implantation damage was annealed by 16 % at a dose of $1.6 \times 10^{17}/cm^2$, which is slightly more than at lower flux for this dose.

### 2.3 $He^+$ Beam Annealing of P implanted diamond.

Although the P implantation damage peak was too deep to measure with a 2 MeV $He^+$ beam, the annealing of the damage near the surface of the crystal could be measured. Due to the drastic effect of swelling induced dechanneling for $He^+$ irradiation, a 120 $\mu$m scan was used, and all data was extracted from the centre of the scans. The diamond was irradiated at a flux of 32 $\mu A/cm^2$ to a maximum dose of $1.6 \times 10^{17}/cm^2$, annealing 21 % of the damage. The spectrum after a dose of only $6.7 \times 10^{16}$ is shown (figure 9), together with the as implanted and unimplanted channeling spectra. This shows that $He^+$ irradiation causes significant annealing at relatively low doses.

The $He^+$ data can be compared to $H^+$ data as long as the damage level is measured over the same physical depth window, as defect dechanneling gives a greater contribution for deeper depth windows. When this analysis was performed, it was found that $He^+$ ions anneal the damage by approximately twice as much as $H^+$ beams at comparable flux.

### 2.4 Conclusions From Annealing Study.

The level of damage is plotted as a function of dose (figure 10) for both of the $H^+$ annealing studies, and the $He^+$ annealing study. The data has been fitted with the function $Y = Y_{eq} \coth(k_1 + k_2 X)$, which is derived from the assumption that the annealing process is a beam induced interstitial/vacancy recombination process [3]. The parameter $k_1$ is related

to the initial defect concentration, and $k_2$ is related to the annealing effect per unit dose. The only parameter that was varied in the least squares fitting to the data was $k_2$. The fit was performed to provide an estimate of the equilibrium damage level $Y_{eq}$. All three studies show that an equilibrium damage concentration $Y_{eq}$ is established at high dose, and that $He^+$ irradiation causes about twice as much annealing than $H^+$ irradiation at high dose, in agreement with the previous study on light ion annealing of ion implanted diamond [5].

The fact that the damage is annealed to an equilibrium value at high dose, rather than completely removed, indicates either that some of the damage exists in types of defects that cannot be annealed by irradiation; or that a dynamic equilibrium is established between defect annealing and defect introduction from the annealing beam The fact that the equilibrium values are beam dependent would tend to support the latter hypothesis. We are presently investigating the effect of ion beam annealing of dopants implanted into diamond.

## 3. Methods for Minimizing Beam induced Changes in Analysis.

In the micro-channeling analysis of unimplanted diamonds, swelling induced dechanneling is the only serious mechanism for channeling loss. Swelling induced dechanneling is more severe for diamond than Si and analysis doses should be kept under $8 \times 10^{16}/cm^2$ to avoid this effect entirely. As this effect is confined to a 10 $\mu$m half width perimeter at the edges of the scan, it can be eliminated from analysis simply by using a larger scan, and extracting data from the central regions of the scan. This allows doses of over $6.0 \times 10^{17}/cm^2$ to be used with negligible channeling loss. This was done in the present 2 MeV $He^+$ annealing study.

Lattice damage from microprobe irradiation could not be measured by channeling for either the $H^+$ beam or the $He^+$ beam, even at the highest doses used in this study. This means that the ultimate limitation on microbeam doses, once edge dechanneling has been eliminated, is the dose at which the irradiated layer is ablated from the surface ($\sim 10^{19}/cm^2$ for Si) [13].

Under poor vacuum conditions ($> 10^{-6}$ torr), an amorphous carbon layer can form on the crystal surface, at a rate proportional to beam dose, which increases the size of the diamond channeling surface peak, inducing some dechanneling [3]. This effect can be greater than lattice damage for some crystals [3], including diamond, so a good vacuum ($\sim 10^{-7}$ torr) is essential for accurate quantitative analysis.

In contrast to the channeling loss, the annealing effect of the analysis beam on implanted diamond poses a serious potential problem for accurate analysis, as annealing occurs rapidly at low doses. This effect has exactly the same type of dose and beam behaviour as damage in crystals like Ge [3], GaAs [2,3], and $Hg_xCd_{(1-x)}Te$ [4], and As dopant displacement in Si [2]. The same strategies can therefore be used to minimize the effect of the beam.

Limiting analysis beam dose is the most obvious means of limiting beam induced changes to the target. For characterizing bulk crystal properties, this is a simple matter of increasing the scan size, but for small features dose cannot be limited without limiting statistical accuracy. Increasing the detector solid angle will improve statistical accuracy, but reduce mass and depth resolution due to kinematic spread [2]. This approach was used successfully in the analysis of laser annealed spots [8], where a detector solid angle of 60 msr was used, giving an overall detector resolution of 24 keV and allowing doses of under $5 \times 10^{16}/cm^2$ to be used, limiting annealing of the implanted crystal to under 5 %.

Another approach to minimizing the effects of damage, that to our knowledge has not been previously proposed, is to extrapolate yield vs dose curves to zero dose by fitting an appropriate function to the curve. Such an approach will provide an accurate numerical estimate of a dopant substitutional fraction or a $\chi_{min}$, and allow the analysis beam effects to be fully characterized.

Unless high depth resolution is required, it is preferable to use low energy $H^+$ ions rather than $He^+$ ions for channeling analysis. Limiting beam flux is also desirable as, like crystal damage, annealing is more severe for higher beam fluxes.

Finally, in any form of microprobe channeling experiment, there is no substitute for actually monitoring the channeling yield from all regions of the sample over the course of the experiment.

This work is part of an ongoing quantitative study of ion irradiation effects and analysis beam induced changes using CCM, and the development of channeling STIM as a means of defect profiling [3].

**Acknowlegements.**

S. P. Dooley wishes to acknowledge financial support from an Australian Postgraduate Research Award. We wish to thank Sue Lane of the Royal Melbourne Institute of Technology for performing the Dektak measurements. This work was supported by a University of Melbourne Special Initiative Grant and an Australian Research Council grant.

**References.**

[1] S. P. Dooley and D N. Jamieson. Nucl. Inst. Meth. B66 (1992) 369.

[2] R. A. Brown, J. C. McCallum and J. S. Williams, Nucl. Inst. Meth. B54 (1991) 197.

[3] S P. Dooley and D N. Jamieson, (in preparation).

[4] S. L. Russo, P. N. Johnston, R. G. Elliman, S. P. Dooley, D. N. Jamieson and G. N. Pain. proc. conf. Ion Beam Modification of Materials, Eindhoven, Holland, to be published (1991).

[5] M. Adel, R. Kalish and V. Richter. J. Mater. Res. 1 (3), May/June 1986.

[6] J. C. McCallum, R. A. Brown, E. Nygren, J. S. Williams and G. L. Olson, Mater. Res. Soc. Symp. Proc. 69 (1986) 305.

[7] S. Prawer, D. N. Jamieson, S. P. Dooley, P. Spizzirri, K. P. Ghiggino and R. Kalish. Fall meeting 1992, MPS Symp. A, in press.

[8] D. N. Jamieson, S. Prawer, S. P. Dooley and R. Kalish. (these proceedings).

[9] J. P. F. Sellschop. in 'The Properties of Diamond.' ed. J. E. Field. Academic Press, 1979. p. 107.

[10] J. F. Prins, T. E. Derry and J. P. Sellschop. Phys. Rev. B. Vol 5 No. 12. (1986) 34.

[11] M. Cholewa, G. Bench, A. Saint and G. J. F Legge. Nucl. Inst. Meth. B56/57 (1991) 795.

[12] C. Ascheron, A. Schindler, R. Flagmeyer and G. Otto, Nucl. Inst. Meth. B36 (1989). 163.

[13] J. C. McCallum, private communication, (1992).

## FIGURES

Figure 1: Profilometer trace (Dektak) over a 32 $\mu$m microbeam scan of <110> oriented diamond showing swelling.

Figure 2: Raman spectrum from the 32 $\mu$m scan of figure 1.

Figure 3: CCM image of a 67 $\mu$m scan to a dose of $6.1\times10^{17}$/cm$^2$ 1.4 MeV $H^+$ showing dechanneling from the scan edges due to tilting of the crystal planes by swelling. A low backscattering yield, from good crystal, shows up as dark, a high yield from dechanneling shows up as bright in this image. It is clear that a significant loss of channeling occurs at the edge of the scan in comparison with the centre of the scan.

Figure 4: CCM image of the swollen left edge of the region in figure 3 with the crystal tilted at 0.5° to the <110> axis showing good channeling into the tilted edges of the original scan (dark region) and dechaneling from the misaligned bulk of the crystal (bright region). The motteled effect is due to a scan artifact.

Figure 5: The effect of the swelling of the diamond on the $\chi_{min}$ within the scan area of figure 3. This has been resolved into the contribution from the centre and swollen scan edge.

Figure 6: The effect of the swelling of the diamond on the $\chi_{min}$ for a 2 MeV $He^+$ beam.

Figure 7: A CCM image of a central 67 $\mu$m, 1.4 MeV $H^+$ scan used to anneal damage in a P implanted diamond (see text).

Figure 8: Channeling spectra extracted from the central 1.4 MeV $H^+$ annealed region and surrounding unannealed, as implanted regions of figure 7.

Figure 9: Channeling spectra from the centre of a 2 MeV $He^+$ annealed region and surrounding unannealed, as implanted diamond.

Figure 10: The damage level (see text) in 1.4 MeV $H^+$ and 2 MeV $He^+$ ion beam annealed diamond as a function of dose fitted with a theoretical curve.

Figure 1: Dooley, Jamieson and Prawer, $He^+$ and $H^+$ Microbeam Damage, Swelling and $He^+$ and H+ Microbeam Damage, Swelling and Annealing in Diamond.

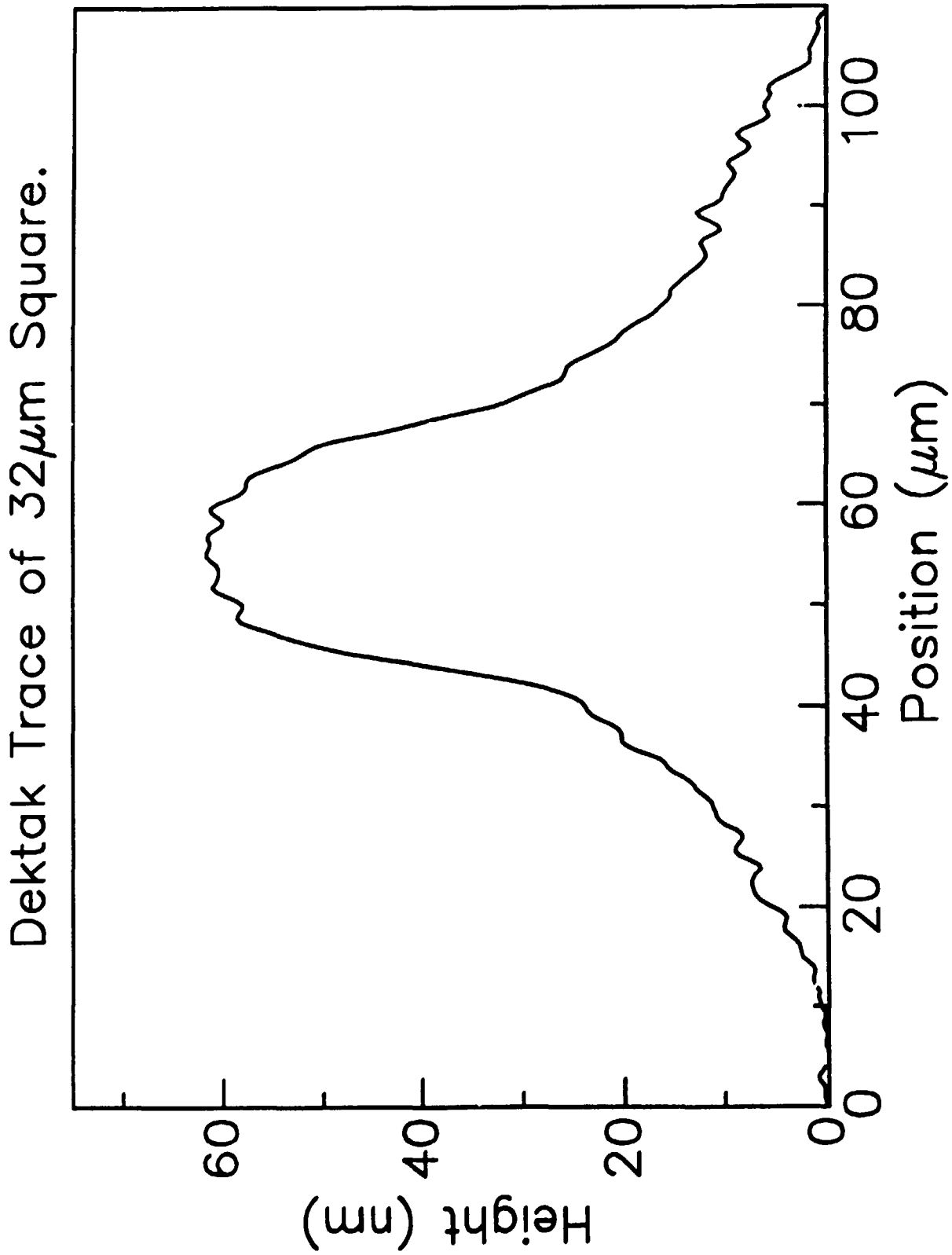

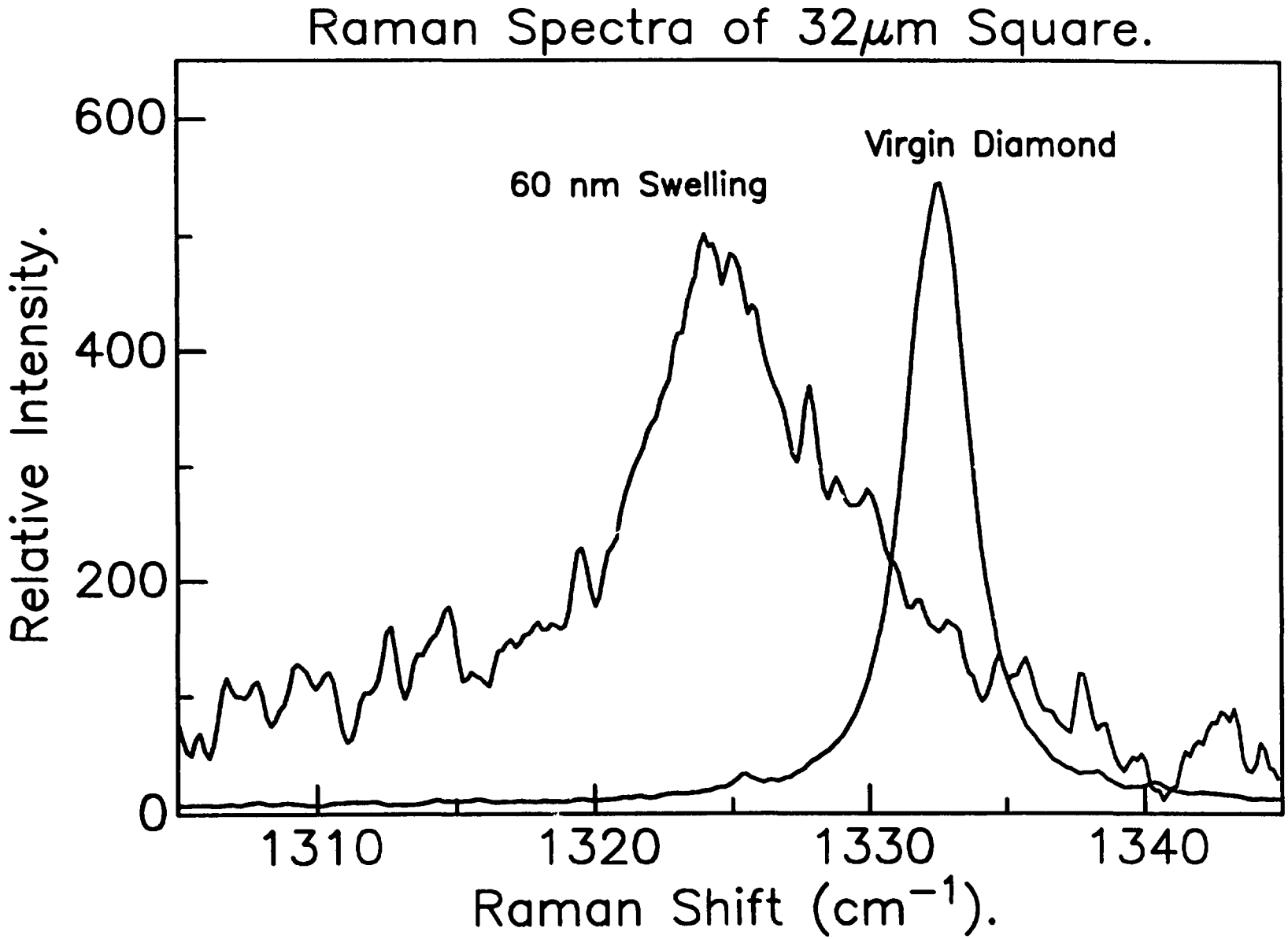


Figure 2. Sean P. Dooley, David N. Jamieson and Steven Prawer, He+ and H+ Microbeam Damage, Swelling and He+ and H+ Microbeam Damage, Swelling and Annealing in Diamond.

Figure 3: Sean P. Dooley, David N. Jamieson and Steven Prawer, $He^+$ and H+ Microbeam Damage, Swelling and $He^+$ and H+ Microbeam Damage, Swelling and Annealing in Diamond.

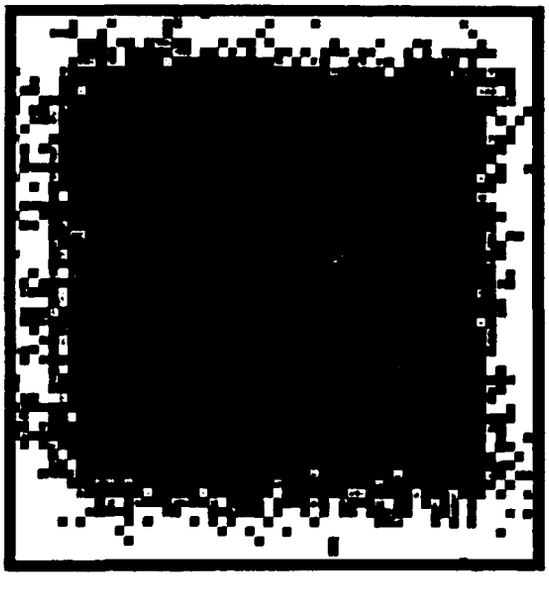

Figure 4: Sean P. Dooley, David N. Jamieson and Steven Prawer, $He^+$ and H+ Microbeam Damage, Swelling and $He^+$ and H+ Microbeam Damage, Swelling and Annealing in Diamond.

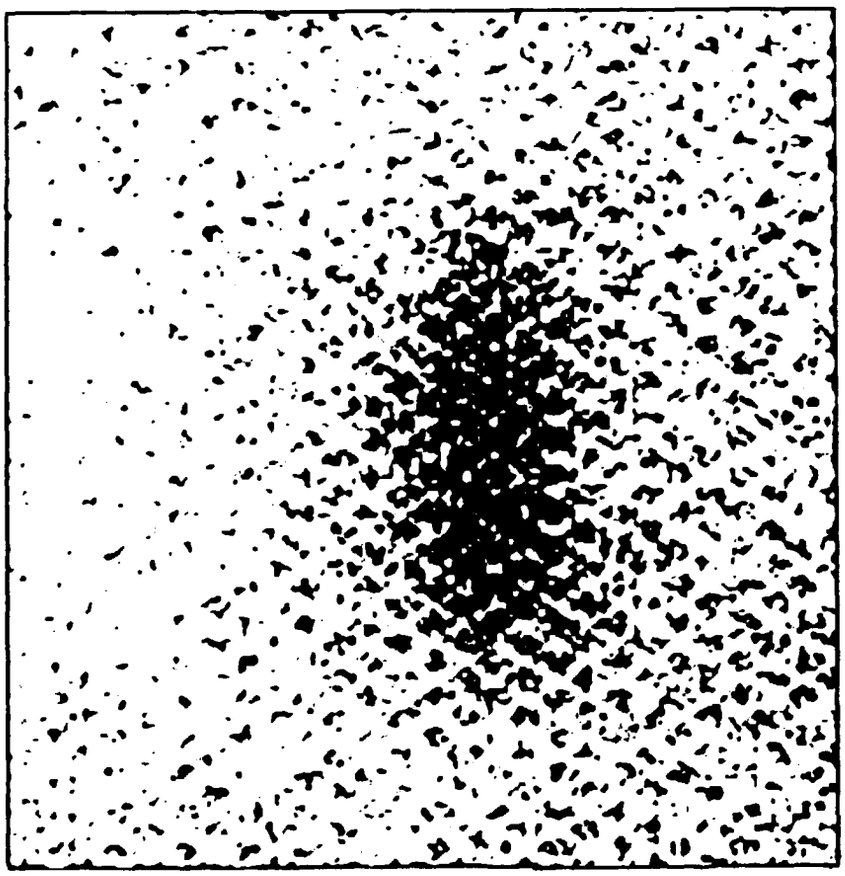

Figure 5: Sean P. Dooley, David N. Jamieson and Steven Prawer, $He^+$ and H+ Microbeam Damage, Swelling and $He^+$ and H+ Microbeam Damage, Swelling and Annealing in Diamond.

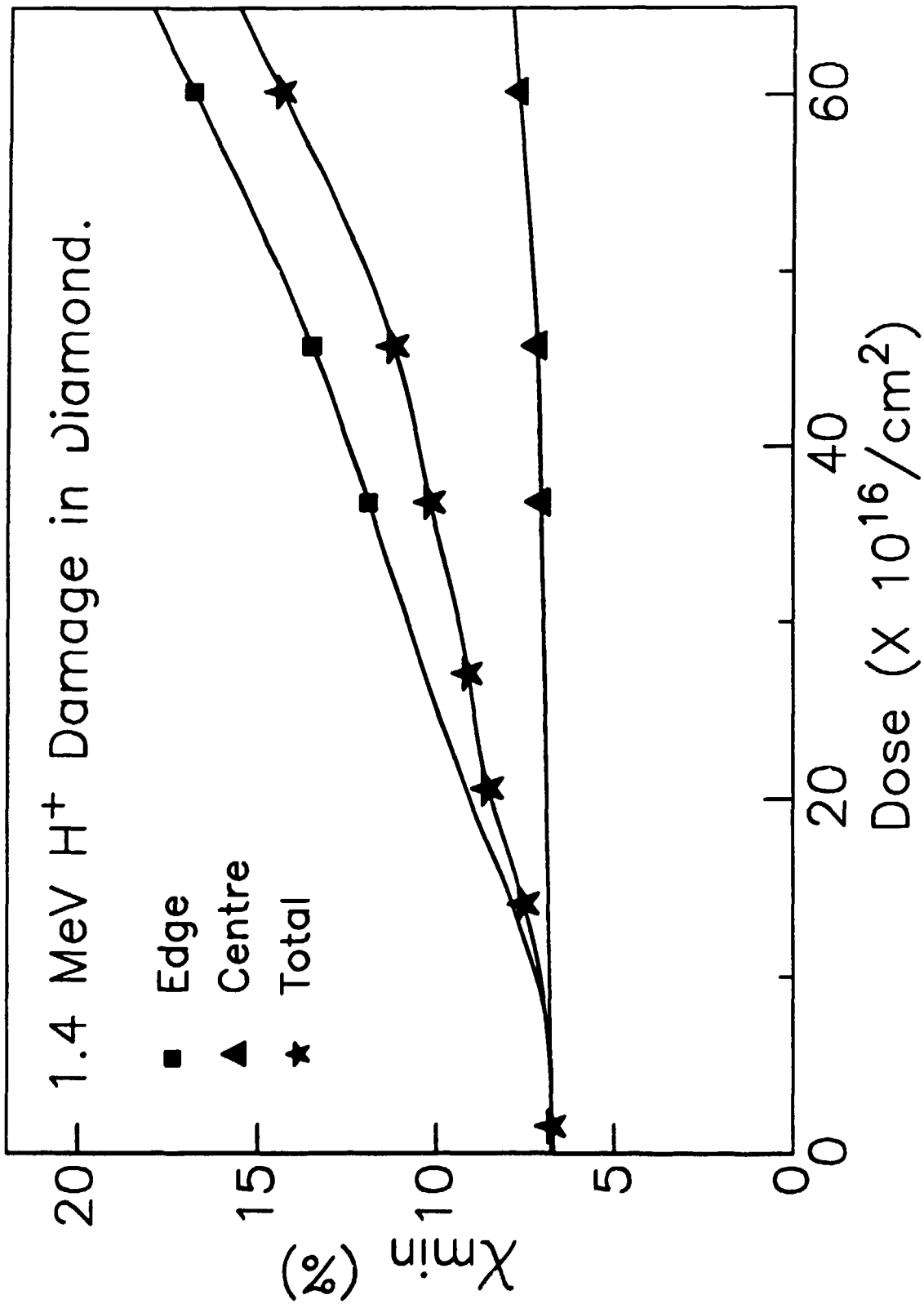

Figure 6: Sean P. Dooley, David N. Jamieson and Steven Prawer, $He^+$ and H+ Microbeam Damage, Swelling and $He^+$ and H+ Microbeam Damage, Swelling and Annealing in Diamond.

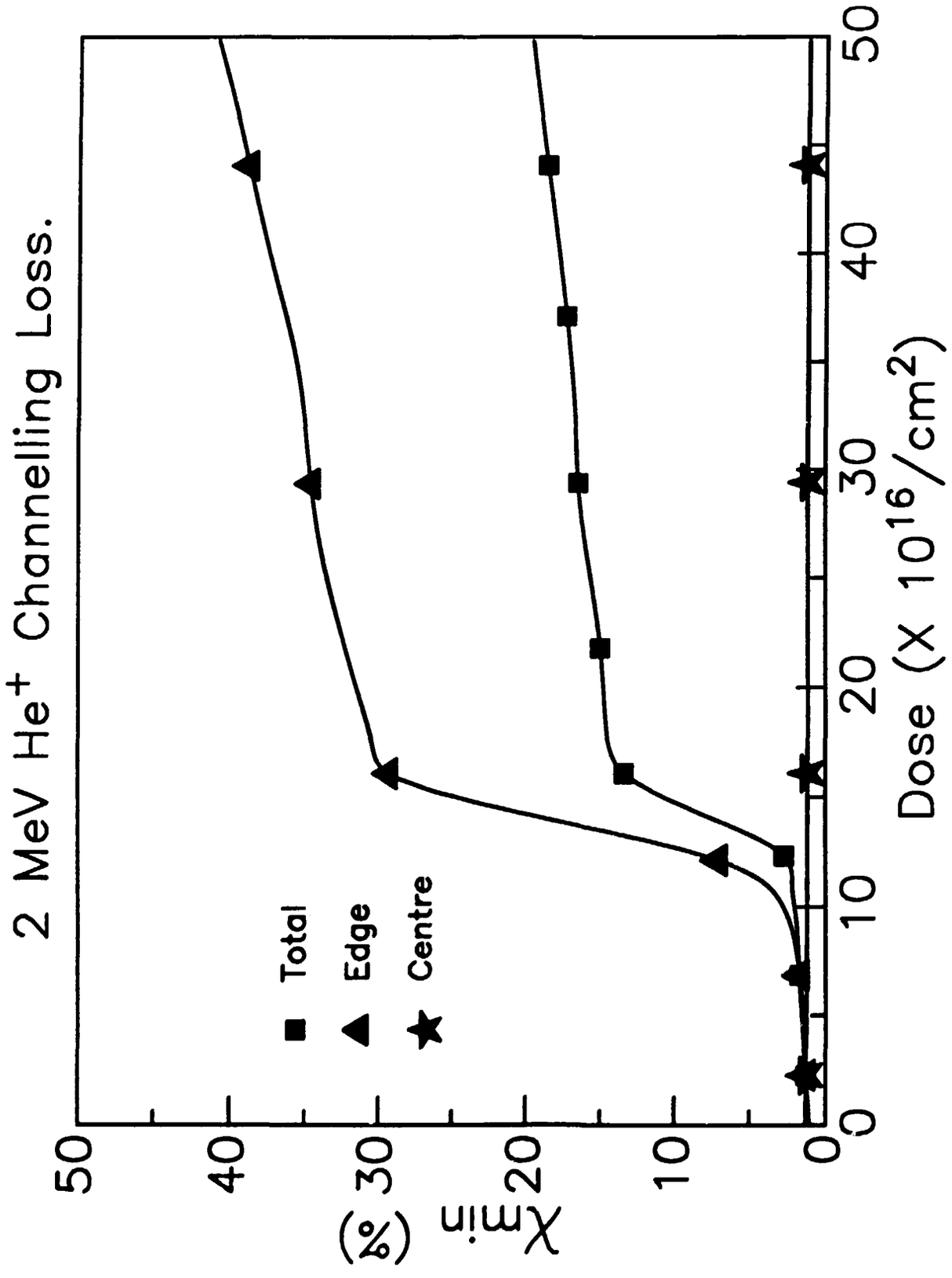

Figure 7: Sean P. Dooley, David N. Jamieson and Steven Prawer, $He^+$ and H+ Microbeam Damage, Swelling and $He^+$ and H+ Microbeam Damage, Swelling and Annealing in Diamond.

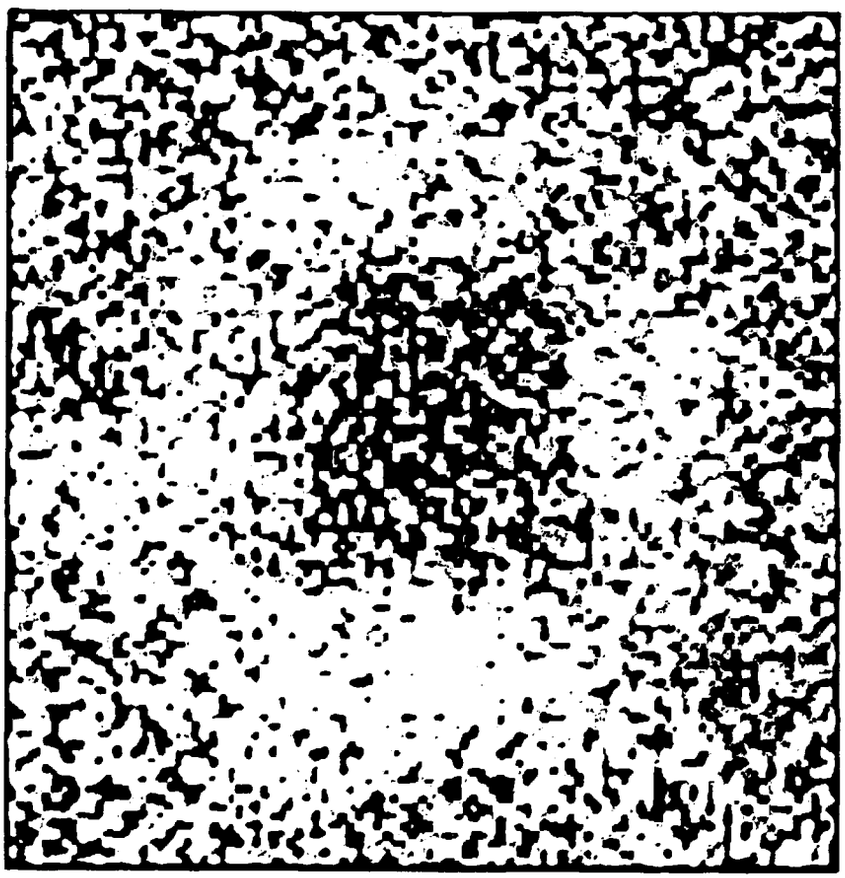

Figure 8: Sean P. Dooley, David N. Jamieson and Steven Prawer, He+ and H+ Microbeam Damage, Swelling and He+ and H+ Microbeam Damage, Swelling and Annealing in Diamond.

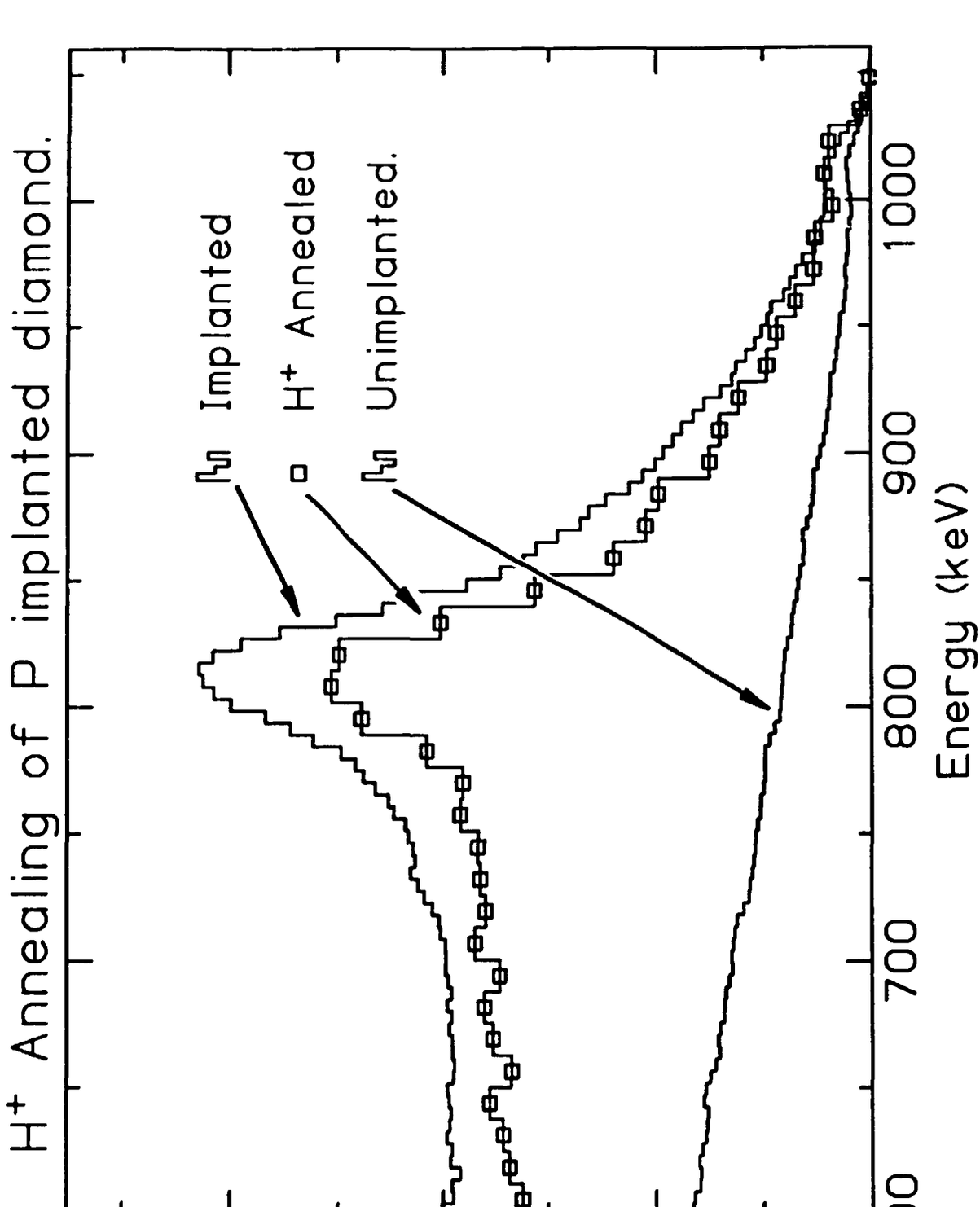

Figure 9: Sean P. Dooley, David N. Jamieson and Steven Prawer, $He^+$ and H+ Microbeam Damage, Swelling and $He^+$ and H+ Microbeam Damage, Swelling and Annealing in Diamond.

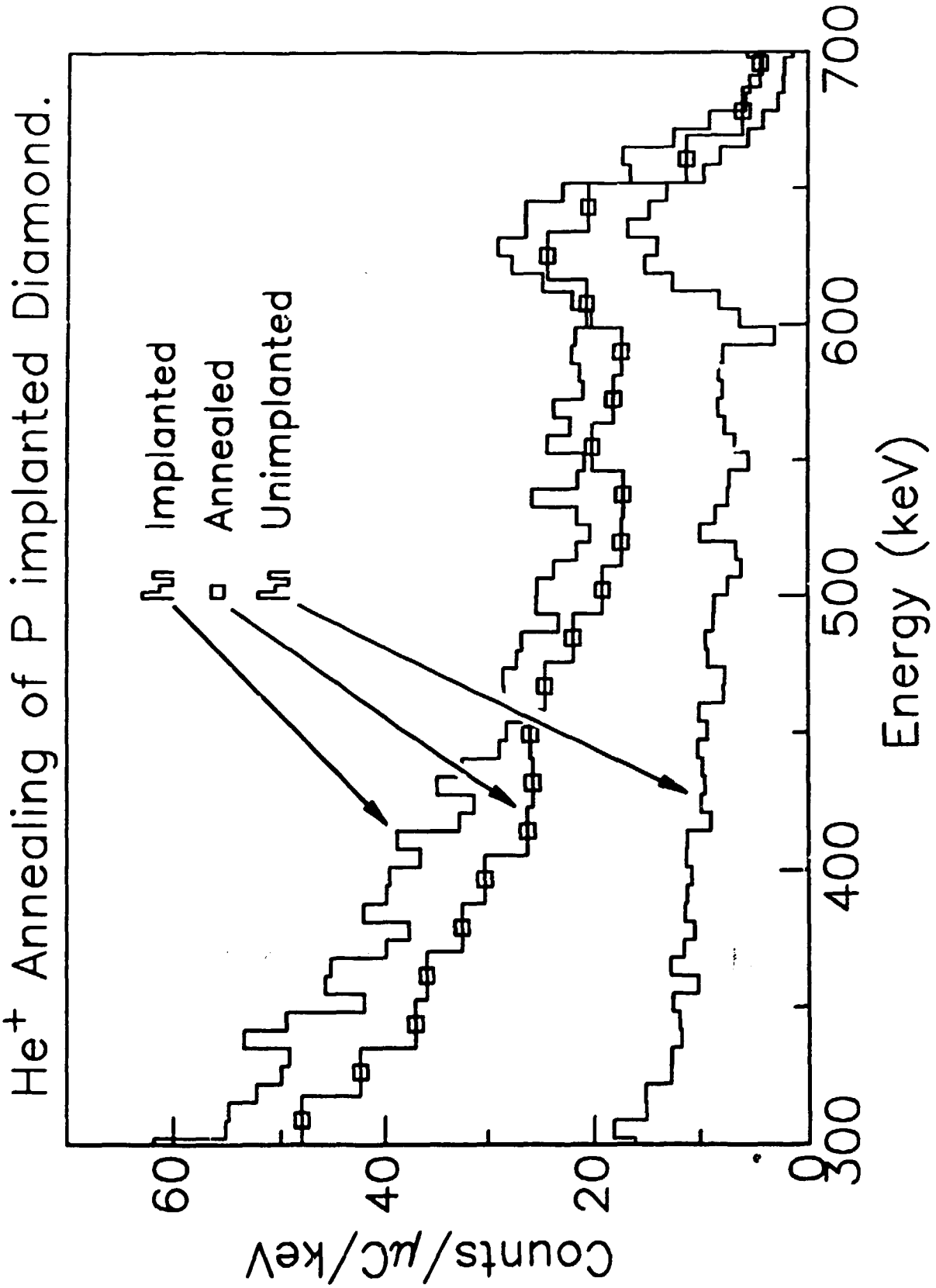

Figure 10: Sean P. Dooley, David N. Jamieson and Steven Prawer, $He^+$ and H+ Microbeam Damage, Swelling and $He^+$ and H+ Microbeam Damage, Swelling and Annealing in Diamond.